

Structural Performance of an Asphalt Pavement Containing Cold Central Plant Recycling and Full-Depth Reclamation

Brian K. Diefenderfer¹, Gerardo Flintsch² , Wenjing Xue³,
Fabrizio Meroni³, Ilker Boz¹ , and David Timm⁴ 

Transportation Research Record
1–11

© National Academy of Sciences:
Transportation Research Board 2022
Article reuse guidelines:

sagepub.com/journals-permissions
DOI: 10.1177/03611981221099511

journals.sagepub.com/home/trr



Abstract

Pavement recycling techniques are often perceived as only applicable to lower traffic volume roadways. However, recent studies have shown their potential for long service lives in higher traffic volume applications. This study documented the response of an asphalt pavement section, constructed using full-depth reclamation (FDR) and cold central plant recycling (CCPR), on a portion of I-64 in Virginia reconstructed between 2016 and 2019. The pavement section was instrumented and the response was compared with a similarly instrumented pavement section (Section S12) placed at the National Center for Asphalt Technology (NCAT) Test Track in 2012. Previous studies have shown that Section S12 is a long-life pavement and it carried 30 million equivalent single axle loads (ESALs) while showing no evidence of deterioration at the pavement surface or from installed instrumentation. The results from the I-64 Segment II project showed that it had much lower horizontal strain values at the bottom of the asphalt layers but slightly higher vertical pressure values on top of the subgrade when compared with NCAT Section S12. Despite the slightly higher values (about 1 pounds per square inch [psi] difference), the vertical pressure on top of the subgrade was very low for both pavement sections. The study confirmed that a recycled pavement section could be constructed and result in low strain and pressure values and is expected to have a long service life in a high traffic volume environment.

Keywords

infrastructure, construction, asphalt pavement construction and rehabilitation, cold in-place recycling, pavements, design and rehabilitation of asphalt pavements, asphalt, pavement design, pavement modeling, pavement structural testing and evaluation, sustainable and resilient pavements, sustainable pavements

Interest in studying and implementing pavement recycling techniques has increased in recent years because of the documented good performance, cost advantages, and environmental benefits of using these processes (1–11). This has coincided with an increased use and study of reclaimed asphalt pavement (RAP) in pavement construction and maintenance also because of its economic and environmental benefits (12). Pavement recycling techniques, including cold in-place recycling (CIR), cold central plant recycling (CCPR), and full-depth reclamation (FDR), have not been used widely on higher traffic volume roadways in the United States because of uncertainty about their long-term performance (3, 13). However, there is growing evidence of good performance using pavement recycling on higher traffic volume roadways (13–16).

In 2016, the Virginia Department of Transportation (VDOT) awarded the contract for reconstruction and new lane addition of a portion of Interstate 64 (I-64) near Williamsburg. The project, having a total contract

¹Virginia Transportation Research Council, Virginia Department of Transportation, Charlottesville, VA

²Center for Sustainable Transportation Infrastructure, Virginia Tech Transportation Institute, The Charles Via, Jr. Department of Civil and Environmental Engineering, Virginia Tech, Blacksburg, VA

³Center for Sustainable Transportation Infrastructure, Virginia Tech Transportation Institute, Blacksburg, VA

⁴Department of Civil and Environmental Engineering, Auburn University, Auburn, AL

Corresponding Author:

Brian K. Diefenderfer, brian.diefenderfer@vdot.virginia.gov

value of approximately \$176 million, was known locally as Segment II because it was the second of a three-part corridor widening/reconstruction sequence (17). The work included reconstructing the existing travel lanes and right shoulder along with adding a third lane and a new left shoulder in both directions for a distance of 7.08 mi. During the early planning stages of the project, a push was made to include pavement recycling techniques as a major component of the Segment II pavement design. Ultimately, FDR and CCPR were included as components of this design.

The recycling-based pavement design for the I-64 Segment II project was based on lessons learned from previous pavement recycling projects in Virginia where CCPR and FDR were combined in one pavement structure. These projects included the portion of I-81 in Augusta County constructed in 2011 (14, 15), shown in Figure 1a, and Section S12 of the VDOT-sponsored sections at the National Center for Asphalt Technology (NCAT) Test Track constructed in 2012 (13, 15, 16) as shown in Figure 1b. The pavement sections on I-81 and Section S12 have carried more than 20 and 30 million ESALs to date, respectively, while showing no deterioration at the pavement surface (15, 16). Given this performance of the NCAT Section S12 design, the pavement section is considered a long-life (perpetual) pavement.

For the I-64 Segment II project, the pavement cross section for both the reconstructed and added lanes was the same and is shown in Figure 1c. The foundation for this design was a 12 in. thick FDR layer. The FDR in the existing lanes was produced from the existing aggregate base and upper portion of the existing subgrade. The FDR in the new lanes was produced from either RAP or recycled concrete aggregate brought to the project from offsite and combined with the existing subgrade; this process is termed here “imported FDR.” The FDR was stabilized using cement at a predominant dosage rate of 4.0%. The dosage rate was selected following a mix design process performed by the contractor; the compressive strength was required to be within the range of 250 to 450 psi. Above the FDR layer, a 2 in. thick layer of an asphalt stabilized open graded drainage layer (OGDL) was used in an effort to improve the subsurface drainage of the pavement structure. On top of the OGDL, a 6 in. thick layer of CCPR was placed. The CCPR was produced using 2.5% foamed asphalt binder and 1.0% cement. The CCPR material was produced using RAP and a common quarry derived material. The CCPR consisted of 85% RAP, sourced from existing regional stockpiles, and 15% #10 aggregates that were considered a quarry co-generated product (i.e., resulting from the production of other desired products) and thus having minor economic value previously. The dosage rate for the CCPR was selected following a mix design process

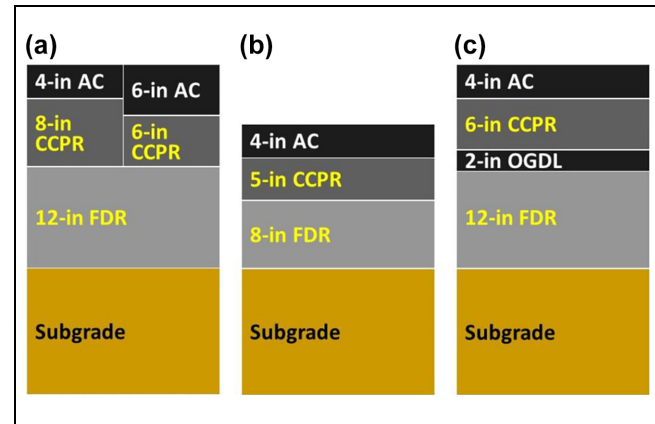


Figure 1. Pavement structures using recycling techniques: (a) I-81, (b) National Center for Asphalt Technology (NCAT) Test Track Section S12, (c) I-64 Segment II.

Note: AC = asphalt concrete, CCPR = cold central plant recycling, OGDL = open graded drainage layer, FDR = full-depth reclamation.

performed by the contractor based on an indirect tensile strength requirement of at least 45 psi. The CCPR gradation included 100% passing the 1.0 in. sieve, 55.8% passing the #4 sieve, and 2.2% passing the #200 sieve. Above the CCPR, two layers of stone matrix asphalt (SMA) were added. The layer immediately above the CCPR was a 2 in. thick layer of SMA having a 19.0 mm nominal maximum aggregate size (NMAS) and a performance grade (PG) 70-22 asphalt binder. The driving surface layer was a 2 in. thick layer of SMA having a 12.5 mm NMAS and a PG 70-22 asphalt binder. The concept of using SMA surface layers, CCPR, and FDR has been proven to provide long-lasting pavement sections in high traffic applications (13–17). Construction of the I-64 Segment II pavement section began in fall 2016 and was completed in fall 2019 (17).

Including pavement recycling in the design of the I-64 Segment II project was another major step forward in the implementation of pavement recycling techniques in the United States and included several unique components. First, this was one of the largest uses of recycled materials on a paving project in the United States; the as-awarded quantities of CCPR and FDR combined were greater than approximately 500,000 tons. Second, the use of #10 aggregates in the CCPR provided the opportunity to utilize a material having minor economic value in a structurally contributing layer. Third, the use of imported FDR on this project is one of the first applications of this technique on the Interstate system in the United States. FDR was usually performed by reclaiming existing pavement foundation materials (3, 18). Lastly, the sections were instrumented during construction with sensors to measure strain, pressure, moisture content, and temperature.

Objectives

The objectives of this study were to assess the early structural performance of the recycled pavement placed on the I-64 Segment II project through instrumentation installed during construction and to compare the response with another similarly constructed pavement section built using pavement recycling techniques. These objectives were accomplished by installing sensors in the roadway that allowed for measurement of the pavement response from truck loading, comparing the strain and pressure response of the I-64 Segment II recycled pavement section completed in 2019 with Section S12 at the NCAT Test Track built in 2012.

Methods

Instrumentation

Pavement sensors were installed during construction to better understand the mechanistic performance of the recycled pavement design used on the I-64 project. The instruments included asphalt strain gauges (Tokyo Sokki Kenkyujo Co. KM-100HAS), pressure cells (Geokon 3500), moisture sensors (Decagon GS1), and thermocouples (Pyromation type T). The instruments were placed in the right wheel path of the right travel lane in the westbound direction just past the ramp to Exit 242B (to northbound Marquis Center Parkway, SR 199) with significant logistical support provided by the prime contractor during installation. All wiring from the sensors was run to a junction box buried at the side of the road. A portable data acquisition system was used to collect the data from all of the instruments.

The instruments were placed in three phases. In the first phase, pressure cells and moisture sensors were

placed on top of and within the subgrade during production of the FDR layer. For the second phase, strain gauges and pressure cells were placed on top of the OGDL layer before placement of the CCPR layer. The third phase of instrumentation was completed after the first SMA layer was placed on top of the CCPR. In the third phase, holes were drilled into the pavement shoulder and a thermocouple tree was installed with thermocouples pre-attached at the desired depths before the application of the surface course. The drilled holes were backfilled with liquid asphalt binder. Figure 2 shows the location of the instruments within the pavement structure.

The pressure cells were placed on top of the subgrade (so they were incorporated into the overlying FDR layer). This was done after a reclaimer had mixed the materials for the FDR layer but before the material was compacted. To place the instruments, their intended location was marked on the surface of the mixed (but not yet compacted) FDR layer with the help of a differential global positioning system (GPS). The instrument position and depth were continually checked as a small excavator was used to dig trenches for the instruments and wiring. All wires were pulled through flexible metal conduit to protect them and were then secured in place using short sections of perforated metal hanger strap (cut to about 4 in. length) and 4 in. long 20d nails. A small amount of bedding sand was placed beneath each pressure cell to provide uniform support and to help level the pressure cell. The sections of hanger strap were used to secure the wiring during placement of the subsequent layer and were added approximately every 3 to 4 ft, oriented perpendicular to the flexible metal conduit, and nailed to the layer below. After all sensors and wiring were arranged and secured, the excavated material

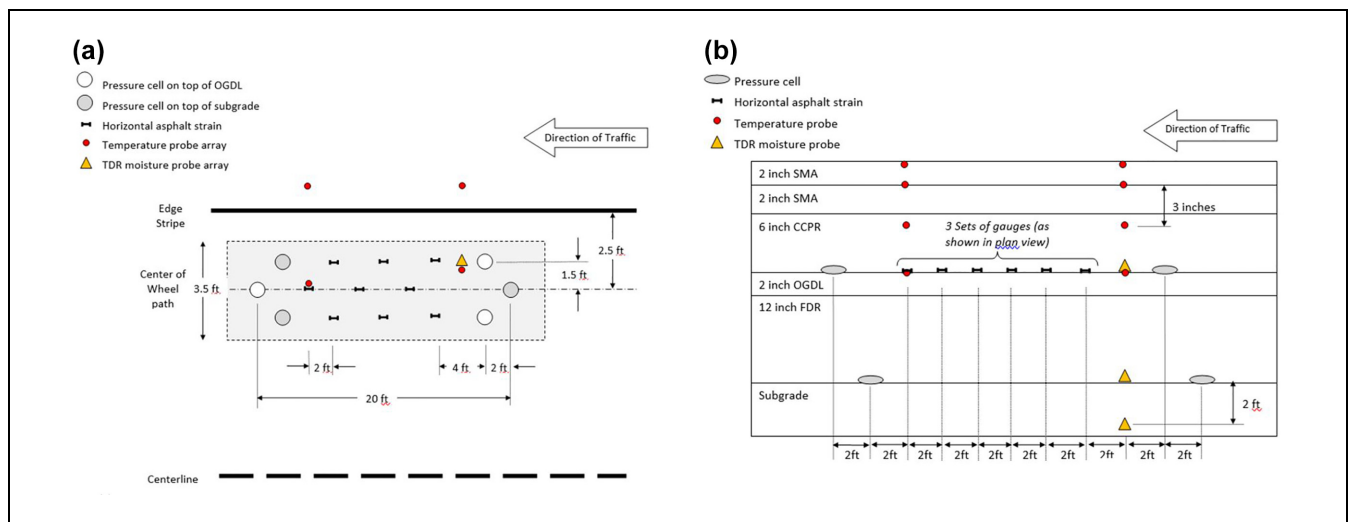


Figure 2. Instrumentation layout: (a) plan view and (b) profile view.

was replaced and the FDR layer was compacted as normal. Based on verbal communication with the contractor, there were no adverse effects on the density achieved within the FDR layer caused by the time required to install the sensors.

As shown in Figures 1 and 2, a 2 in. thick asphalt stabilized OGDG layer was paved on top of the FDR layer to provide drainage for the pavement system. The OGDG was connected to longitudinal edge drains that were trenched along the edge of the pavement after the instrumentation was placed in the FDR layer. To account for the trenching, the instrumentation wires were installed several feet below the surface of the subgrade layer at the pavement shoulder so that the longitudinal edge drain could pass above the wiring without severing them when the trench was installed.

Strain gauges were placed on top of the OGDG layer, the day after it was paved, so that the sensors would be incorporated into the bottom of the CCPR layer. To place the strain gauges, their intended location was marked on the OGDG surface with the help of a differential GPS and the sensors were arranged at their approximate locations. The wires for each sensor were then pulled through the protective flexible metal conduit. The sections of hanger strap and 20d nails were again used to secure the conduit to the OGDG but the last 4 to 5 ft of wiring next to the instruments was left unsecured. The strain gauges were seated on the OGDG surface in a thin mastic of sand and heated asphalt binder. Once the mastic had cooled, the last section of wiring was secured. The CCPR layer was then paved, covering over the instruments, with the researchers and the paving crew working to ensure that the dump trucks delivering material to the paver and the paver itself did not run their loaded tires directly on the sensors. Usually, the strain at the bottom of the asphalt layers would be of interest when instrumenting an asphalt pavement. However, since the OGDG layer was only 2 in. thick, the 1/2 in. thick strain gauges were placed on top of this layer so that their placement did not disrupt the construction of the OGDG layer. The maximum strain of the pavement section (located at the bottom of the OGDG layer) was later calculated by modeling as described in the following sections.

As shown in Figure 2, all the instruments, with the exception of the thermocouples, were placed in three lines, parallel to the direction of traffic that covered the left, center, and right portion of the right wheel path in the right travel lane. Using this array of sensors, the peak responses were captured given normal amounts of wandering. Figure 3 presents an overview of the instrumentation process.

Pavement Response

Loaded trucks having known axle weights were driven over the instrumented section on five dates between June and December 2018. For each test date, a series of two- and three-axle VDOT dump trucks were loaded with aggregate and weighed. The trucks were weighed using a series of mobile load scales such that each half axle was weighed simultaneously. The average loaded weight of the two- and three-axle dump trucks was approximately 32,000 lb-m and 45,000 lb-m, respectively.

The trucks were driven by VDOT employees over the instrumented section as part of the public traffic stream. For each test date, between 12 and 20 passes were made by each truck. The instrumentation response during each pass was recorded by a portable data acquisition system located at the side of the road. Since the test trucks were part of the public traffic stream, the researchers used a video camera, having a time stamp synchronized with the data acquisition system, to determine when the test truck crossed the instrumented section, as shown in Figure 4. In this paper, the strain and pressure responses are presented.

Modeling

The maximum strain in an asphalt pavement (consisting of a stiff asphalt layer[s] over a less stiff foundation) is known to occur at the bottom of the bound asphalt layers. For the case of the I-64 Segment II project, the maximum strain was expected at the bottom of the OGDG layer. As mentioned previously, the strain gauges could not be placed at this depth for constructability concerns. Therefore, layered elastic analysis software was used to model the pavement section and calculate the strain at the bottom of the OGDG layer by comparing the modeled and the measured strain slightly above this location within the pavement structure.

The layered elastic analysis was performed by first determining appropriate stiffness values for each layer using the results from previous studies (19–21). These stiffness values were used to seed the model and then calculate the strain at the bottom of the CCPR layer where the strain gauges were installed on the project. The material stiffness inputs were adjusted in an iterative process to reduce the difference between the calculated and the measured strain values. Once the difference between the measured and calculated strains was minimized and the model was considered representative, the calculated strain at the bottom of the OGDG layer was compared with measured strain values from other similar recycled pavement structures.



Figure 3. Instrumentation installation process: (a) full-depth reclamation placement, (b) installing sensors in trenched locations, (c) compacting full-depth reclamation over instruments, (d) marking locations on open-graded drainage layer, (e) close-up of strain gauge, and (f) completed array on open-graded drainage layer.

Results and Discussion

Pavement Response—Tensile Strain (Bottom of CCPR Layer)

From the data collected at each test date, a representative tensile strain value at the bottom of the CCPR layer was calculated as follows: (i) the 95th percentile tensile strain was calculated for the strain gauge having the greatest average strain from all the repeated runs, (ii) the 95th percentile tensile strain was normalized with respect to load, and (iii) the load normalized 95th percentile tensile strain was normalized with respect to temperature.

The strain from each gauge for each single axle pass was determined by taking the difference of the maximum and minimum strain (peak to trough). The 95th

percentile tensile strain was calculated from the replicate passes at the single strain gauge having the highest average tensile strain from all passes. Following this, the 95th percentile tensile strain value was normalized with respect to load by multiplying the 95th percentile tensile strain by the ratio of 20,000 lb divided by the measured axle load. Next, the load normalized 95th percentile tensile strain was normalized with respect to temperature. This was accomplished by plotting the load normalized 95th percentile tensile strain from each measurement date with respect to mid-depth pavement temperature. An exponential trend line was fit to the data, as shown in Figure 5, and the exponent (k_2) from Equation 1 was used in Equation 2 to calculate the temperature normalized tensile strain as follows:



Figure 4. Three-axle truck crossing over instrumented section.

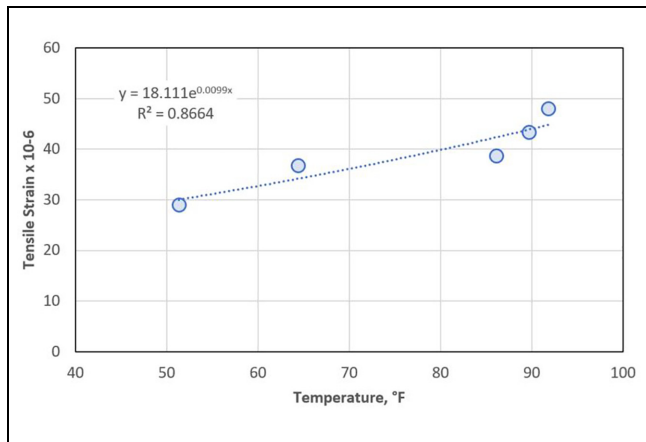


Figure 5. Load normalized 95th percentile tensile strain at the bottom of the cold central plant recycling (CCPR) layer versus mid-depth pavement temperature and an exponential trend line.

$$y = k1 \left(e^{k2(x)} \right) \quad (1)$$

where y = strain, $k1$ and $k2$ = coefficients determined from an exponential trend line, and x = temperature.

$$TNS_{95} = LNS_{95} \left(e^{k2(T_{ref} - T_{MD})} \right) \quad (2)$$

where TNS_{95} = temperature normalized 95th percentile tensile strain, LNS_{95} = load normalized 95th percentile tensile strain, T_{ref} = reference temperature (68°F), and T_{MD} = mid-depth temperature.

The progression from 95th percentile strain to load and temperature normalized 95th percentile tensile strain is shown in Table 1. The results in Figure 5 and Table 1 both show that despite the restraining effects of the FDR layer, the strain response of the pavement structure is still temperature dependent.

The load and temperature normalized 95th percentile tensile strain values are shown in Figure 6. An average

tensile strain value was calculated as 35.5×10^{-6} and became the target for the layered elastic analysis discussed in the following sections. From Figure 6, the tensile strain was found to be nearly constant with respect to time. Some variability was expected and could be attributed to trucks applying the load to the pavement section that may not have crossed directly over the instruments. Maintaining positional alignment was difficult since guiding markers on the roadway were not used. Figure 6 also shows that the tensile strain magnitude was very low and well below even conservative estimates of an asphalt mixture endurance limit (22–24). However, it is not yet known if the endurance limit concept is applicable to cold recycled materials.

Pavement Response—Vertical Subgrade Pressure

Because of the very low signal-to-noise ratio of the pressure cells, the pressure response at the top of the subgrade layer was only available for the first two test dates. Thus, the pressure response was not temperature normalized. The pressure from each pressure cell for each single axle pass was determined as the maximum value recorded. Similar to the strain response, the 95th percentile pressure was calculated from the replicate passes at the single pressure cell having the highest average pressure from all passes. Next, the 95th percentile pressure was normalized with respect to load by multiplying the 95th percentile pressure by the ratio of 20,000 lb divided by the measured axle load and is shown in Figure 7. Since only two measurements were available, the load normalized 95th percentile pressure was not temperature normalized.

Modeling

As stated previously, the strain value from the bottom of the CCPR layer was measured for this pavement section because of constructability concerns. Since the maximum strain was expected to occur at the bottom of the OGDL layer (the layer beneath the CCPR), the maximum strain within the asphalt layers for the pavement section was determined by modeling.

The I-64 Segment II pavement section was modeled using a layered elastic analysis software (WESLEA for Windows). The primary inputs were the thickness and modulus value for each layer (shown in Figure 1 and Table 2, respectively) and the tire load (5,000 lb). The initial modulus values for each layer were taken from the results of other studies (19–21) (subgrade values were obtained from initial design reports) and input into the software as ranges that were varied in a series of trials. The modeled strain values were compared with the measured average tensile strain shown in Figure 6

Table 1. Summary of Collected and Calculated Strain Responses at the Bottom of the Cold Central Plant Recycling Layer

Test date	95th percentile tensile strain, $\times 10^{-6}$	Axle load, lb	Load normalized 95th percentile tensile strain, $\times 10^{-6}$	Mid-depth temperature, °F	Load and temperature normalized 95th percentile tensile strain, $\times 10^{-6}$
6/26/2019	48.0	20,000	48.0	91.9	37.9
8/15/2019	41.8	19,300	43.3	89.7	34.9
9/11/2019	38.1	19,900	38.7	86.1	32.3
11/6/2019	34.5	18,800	36.7	64.4	38.0
12/18/2019	28.0	19,300	29.0	51.4	34.2

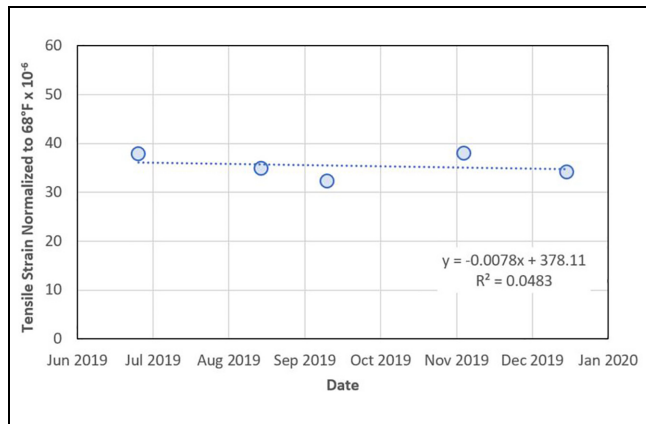


Figure 6. Load and temperature normalized 95th percentile tensile strain at the bottom of the cold central plant recycling layer versus date.

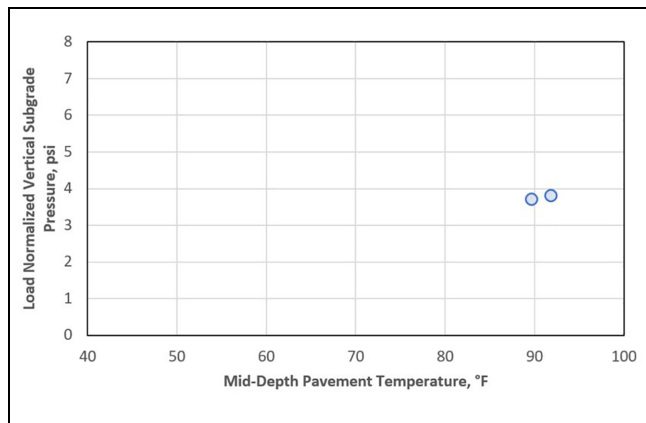


Figure 7. Vertical subgrade pressure versus mid-depth temperature.

(35.5×10^{-6}). When the modeled strain was close to the measured strain, the model inputs were considered appropriate.

After comparing the modeled strains using the inputs shown in Table 2, a revised set of model inputs was developed to further reduce the error between modeled

and measured strain. Table 3 shows the revised model inputs and the output strain values. As shown in Table 3, the modulus values shown for Revised Trial #4 yielded a modeled strain that matched the average measured strain (35.5×10^{-6}) and this combination of modulus values was taken to be representative of the pavement structure. Using the Revised Trial #4 inputs, the calculated strain at the bottom of the OGDL layer was taken to be 39.0×10^{-6} .

Figure 8 shows the strain distribution with respect to pavement thickness for the I-64 Segment II pavement structure using the results of Revised Trial #4. As expected, local maximum tensile strain values were found at the layer interfaces where the material stiffness decreases from one layer to the next. The maximum tensile strain in the entire structure was found at the FDR/subgrade interface. This suggests that the CCPR layer should not experience deterioration by bottom-up fatigue cracking but that the FDR material could if it has brittle behavior.

Comparison With NCAT Section S12

The measured and modeled tensile strains from the I-64 Segment II pavement section were compared with the strain values from a similarly instrumented pavement section—Section S12 built at the NCAT Test Track in 2012 (shown in Figure 1). Figure 9 shows the measured tensile strain with respect to mid-depth temperature at the bottom of the CCPR layer for the I-64 Segment II project and NCAT Section S12 (the tensile strain at the bottom of the OGDL layer for the I-64 Segment II project is not shown since the layer modulus values used in modeling were not considered at multiple temperatures). The tensile strain from NCAT Section S12 was selected from data collected between September 2020 and January 2021 to cover the range of mid-depth pavement temperatures observed at the I-64 Segment II project. As can be seen in Figure 9, the tensile strain at the bottom of the CCPR layer for the I-64 Segment II project is less than the tensile strain at the bottom of the CCPR layer for NCAT Section S12 across the temperature range shown. Even

Table 2. Initial Model Inputs

Range	Modulus values, psi				
	AC	CCPR	OGDL	FDR	Subgrade
High	1,100,000	550,000	550,000	375,000	7,000
Medium	900,000	400,000	400,000	150,000	
Low	800,000	300,000	250,000	100,000	

Note: AC = asphalt concrete, CCPR = cold central plant recycling, OGDL = open graded drainage layer, FDR = full-depth reclamation; psi = pounds per square inch.

Table 3. Revised Model Inputs and Results

Revised trial	Modulus values, psi					Longitudinal tensile strain, 10^{-6}	
	AC	CCPR	OGDL	FDR	Subgrade	Bottom of CCPR	Bottom of OGDL
1	900,000	650,000	300,000	150,000	7,000	35.15	38.54
2				100,000		41.24	49.52
3		600,000	325,000	150,000		34.52	39.00
4			300,000			35.50	38.99
5			275,000			36.56	38.91
6	800,000	650,000	300,000	100,000		41.65	50.07

Note: AC = asphalt concrete, CCPR = cold central plant recycling, OGDL = open graded drainage layer, FDR = full-depth reclamation; psi = pounds per square inch.

when considering the modeled strain at the bottom of the OGDL layer for the I-64 Segment II project shown in Table 3, the measured strain at the bottom of the CCPR layer for NCAT Section S12 is still much greater. The excellent performance of Section S12 through 30 million ESALs (15, 16) suggests that Section S12 is a perpetual pavement structure. If the I-64 Segment II structure follows a similar performance, it too could be a perpetual structure.

The difference in strains between I-64 Segment II and NCAT Section S12 is thought to be caused by the additional thickness (both CCPR and FDR layers) of the pavement section of the I-64 Segment II project as compared with the NCAT Section S12 cross section (shown in Figure 1). As shown in Figure 9, the tensile strain from NCAT Section S12 has a greater change over a similar temperature range the tensile strain from the I-64 Segment II project. Using the regression models shown in Figure 9, the expected tensile strain at 68°F for NCAT Section S12 was about 3.5 times the tensile strain measure at the I-64 Segment II project.

Figure 10 shows the vertical subgrade pressure with respect to mid-depth temperature for the I-64 Segment II project and NCAT Section S12. The vertical subgrade pressure from NCAT Section S12 was taken from data collected between September 2020 and January 2021 (the same dates as the strain shown in Figure 9). Figure 10

shows only two data points for the I-64 Segment II project. This is because the noise in the pressure cell response exceeded the signal response from traffic loading after the first two measurement dates. Figure 10 shows that the vertical subgrade pressure from the I-64 Segment II project was slightly higher than the vertical subgrade pressure from NCAT Section S12. The reason for this difference is unknown since both locations conducted testing using axle loads of approximately 20,000 lb. However, for both projects, the vertical subgrade pressure is very low and the difference between the projects is not considered significant (less than approximately 1 psi at similar temperatures). Using the regression model shown in Figure 10, the expected subgrade pressure at NCAT Section S12 at 90°F was approximately 2.8 psi. By comparison the measured subgrade pressure at the I-64 Segment II project at 89.7°F was 3.7 psi.

Performance Implications for I-64 Segment II

Comparing the calculated tensile strain for I-64 Segment II and the measured strain at NCAT Section S12 showed that the I-64 section had a lower tensile strain value. Conventional pavement design theory suggests that the section having lower strain values at the bottom of the asphalt layers should have a longer service life by resisting damage from bottom-up fatigue cracking. If this

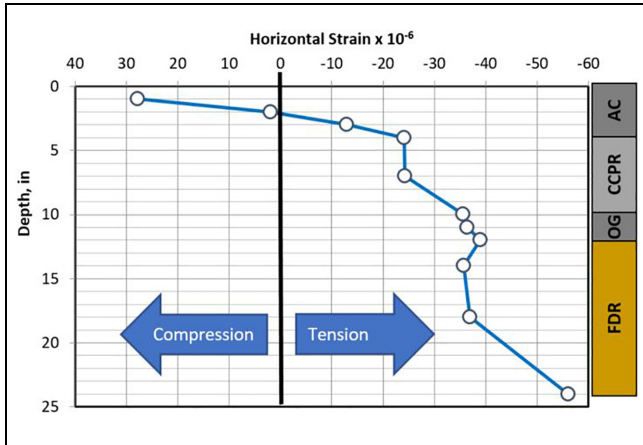


Figure 8. Strain distribution with respect to depth.
 Note: AC = asphalt concrete, CCPR = cold central plant recycling, OGDL = open graded drainage layer, FDR = full-depth reclamation.

holds true for recycled pavement materials, then either design would be highly advantageous for agencies since addressing the cause of deterioration from bottom-up fatigue failure often includes deep rehabilitation. By eliminating fatigue-related deterioration, pavement rehabilitation will more likely be confined to the upper layers of the pavement structure where repairs can be made with less user delays and at lower costs (15, 22, 25, 26).

Unfortunately, there is little information available in the literature to document the fatigue response of CCPR materials to confirm the assumptions listed above. Until this information (including performance models) becomes available, researchers can assume the same logic as used for dense-graded asphalt mixtures. However, as stated by Diefenderfer et al. (16), NCAT Section S12 featuring CCPR placed over an FDR foundation exhibited excellent performance through 30 million ESALs at strain levels where previously-constructed test sections containing dense-graded asphalt mixtures have begun to experience bottom-up fatigue damage.

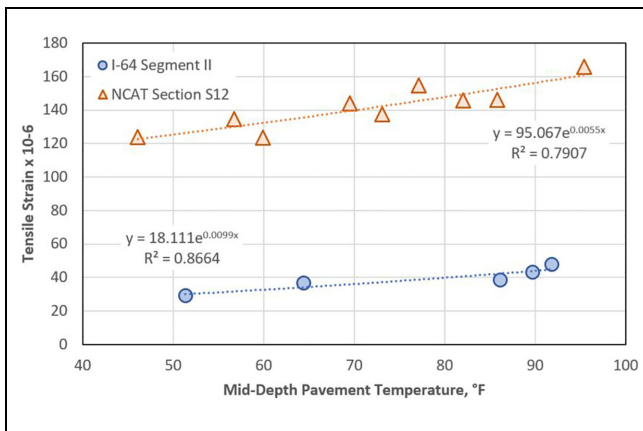


Figure 9. Measured tensile strain of I-64 Segment II and National Center for Asphalt Technology (NCAT) Section S12 versus mid-depth temperature.

The I-64 Segment II project had a calculated tensile strain value that was less than that typically given as the endurance limit for asphalt mixtures. From this strain-based perspective, the design of the I-64 Segment II project could probably be optimized to allow a higher strain given the excellent field performance of the NCAT Section S12 design (16). However, it is not known what implications this might have with respect to the modeled strain at the bottom of the FDR layer (shown in Figure 8) if the overall structure were made thinner or the shear performance at the top of the CCPR layer if the asphalt surface were thinner.

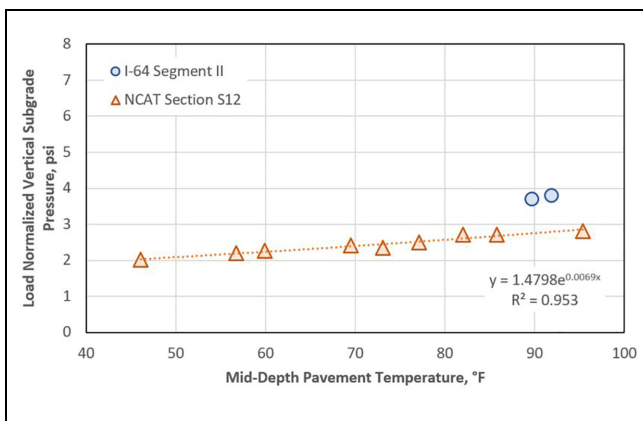


Figure 10. Pressure at I-64 Segment II and National Center for Asphalt Technology (NCAT) Section S12 versus mid-depth temperature.

The long-term performance of recycled pavements, especially when techniques are combined like the examples shown in this study, is not well documented outside research projects in Virginia and at the NCAT Test Track. It is unclear what other potential modes of failure in the CCPR layer (or the FDR layer) are likely since rutting (from densification or shear) also does not appear to be prevalent provided the CCPR layer is designed and constructed properly and a sufficiently thick asphalt surfacing is included. One area of potential future study could be to investigate the fatigue performance of the FDR layer where the highest strain in the Segment II pavement section was found, as shown in Figure 8. Fatigue of the FDR layer could be a concern for thinner FDR layers, but it is not expected for the thicker structure used on I-64 Segment II.

Findings and Conclusion

- A pavement structural design that relies heavily on recycled materials (e.g., CCPR and FDR) can

yield a low-strain pavement section likely having perpetual performance.

- Use of the FDR layer is credited with controlling the strain in the overlying asphalt layers.
- The pavement design used on the I-64 Segment II that used FDR and CCPR to incorporate significant proportions of recycled materials into the pavement structure was found to have both low strain and low pressure values at early stages of the pavement life.
- Layered elastic modeling can be used to calculate strain values in locations that are different from where strain sensors were installed.
- The strain calculated at the bottom of the CCPR layer was well below even conservative estimates of an endurance limit for asphalt mixtures. It is not yet known if the endurance limit concept is applicable to cold recycled materials.
- The expected low strain and pressure values resulting from the FDR/CCPR design were confirmed and a long service life is expected based on comparison with other similar projects.
- The benefits of using pavement recycling techniques can be realized in high traffic locations by using a pavement design similar to the I-64 Segment II project.

Acknowledgments

The authors appreciate the support and assistance from Thomas Tate, Girum Merine, James Peavy, and Affan Habib, Virginia Department of Transportation; personnel from Allan Myers, Inc.; and Benjamin Bowers, Auburn University.

Author Contributions

The authors confirm contribution to the paper as follows: study conception and design: B. Diefenderfer, G. Flintsch, D. Timm; data collection: G. Flintsch, W. Xue, F. Meroni, B. Diefenderfer, I. Boz; analysis and interpretation of results: B. Diefenderfer, G. Flintsch, W. Xue, F. Meroni, D. Timm, I. Boz; draft manuscript preparation: B. Diefenderfer, G. Flintsch, W. Xue, F. Meroni, D. Timm, I. Boz. All authors reviewed the results and approved the final version of the manuscript.


Declaration of Conflicting Interests


The author(s) declared no potential conflicts of interest with respect to the research, authorship, and/or publication of this article.


Funding

The author(s) received no financial support for the research, authorship, and/or publication of this article.

ORCID iDs

Gerardo Flintsch  <https://orcid.org/0000-0003-4440-0711>

Ilker Boz  <https://orcid.org/0000-0002-8534-6996>

David Timm  <https://orcid.org/0000-0001-5719-2523>

References

1. Atkins, A. E., B. Lane, and T. Kazmierowski. Sustainable Pavements: Environmental, Economic, and Social Benefits of in Situ Pavement Recycling. *Transportation Research Record: Journal of the Transportation Research Board*, 2008. 2084: 100–103.
2. Chiu, C. T., T. S. Hsu, and W. F. Yang. Life Cycle Assessment on Using Recycled Materials for Rehabilitating Asphalt Pavements. *Resources, Conservation and Recycling*, Vol. 52, 2008, pp. 545–556.
3. Stroup-Gardiner, M. *Recycling and Reclamation of Asphalt Pavements Using In-Place Methods*. NCHRP Synthesis 421. National Cooperative Highway Research Program, Washington, D.C., 2011.
4. Aurangzeb, Q., and I. L. Al-Qadi. Asphalt Pavements With High Reclaimed Asphalt Pavement Content: Economic and Environmental Perspectives. *Transportation Research Record: Journal of the Transportation Research Board*, 2014. 2456: 161–169.
5. Giani, M. I., G. Dotelli, N. Brandini, and L. Zampori. Comparative Life Cycle Assessment of Asphalt Pavements Using Asphalt, Warm Mix Technology, and Cold In-Place Recycling. *Resources, Conservation and Recycling*, Vol. 104, 2015, pp. 224–238.
6. Santos, J., J. Bryce, G. Flintsch, A. Ferreira, and B. Diefenderfer. A Life Cycle Assessment of In-Place Recycling and Conventional Pavement Construction and Maintenance Practices. *Structure and Infrastructure Engineering*, Vol. 11, 2015, pp. 1199–1217.
7. Santos, J., G. Flintsch, and A. Ferreira. Environmental and Economic Assessment of Pavement Construction and Management Practices for Enhancing Pavement Sustainability. *Resources, Conservation and Recycling*, Vol. 116, 2017, pp. 15–31.
8. Arimilli, S., M. N. Nagabhushana, and P. K. Jain. Comparative Mechanistic-Empirical Analysis for Design of Alternative Cold Recycled Asphalt Technologies With Conventional Pavement. *Road Materials and Pavement Design*, Vol. 19, 2018, pp. 1595–1616.
9. Al-Qadi, I. L., H. Ozer, B. Diefenderfer, and Q. Zhou. Pavement Recycling: A Case Study of Life-Cycle Assessment and Life-Cycle Cost Analysis. *Proc., 2020 Conference on Pavement, Roadway, and Bridge Life Cycle Assessment*, Sacramento, CA, 2020.
10. Amarh, E., J. Santos, G. Flintsch, and B. Diefenderfer. Development of Pavement Performance Prediction Models for in Situ Recycled Pavements in Virginia. *Proc., 2020 Conference on Pavement, Roadway, and Bridge Life Cycle Assessment*, Sacramento, CA, 2020.
11. Al-Qadi, I. L., and H. Ozer. *In-Place and Central-Plant Recycling of Asphalt Pavements in Virginia*. FHWA-HIR-19-078. Federal Highway Administration, Washington, D.C., 2020.

12. Williams, B. A., J. R. Willis, and J. Shacat. *Asphalt Pavement Industry Survey on Recycled Materials and Warm-Mix Asphalt Usage 2019*. National Asphalt Pavement Association, Greenbelt, MD, 2019.
13. Timm, D. H., B. K. Diefenderfer, and B. F. Bowers. Cold Central Plant Recycled Asphalt Pavements in High Traffic Applications. *Transportation Research Record: Journal of the Transportation Research Board*, 2018. 2672: 291–303.
14. Diefenderfer, B. K., B. F. Bowers, and A. K. Apeagyei. Initial Performance of Virginia's Interstate 81 In-Place Pavement Recycling Project. *Transportation Research Record: Journal of the Transportation Research Board*, 2015. 2306: 21–27.
15. Timm, D. H., B. K. Diefenderfer, B. F. Bowers, and G. F. Flintsch. Utilization of Cold Central Plant Recycled Asphalt in Long-Life Flexible Pavements. *Transportation Research Record: Journal of the Transportation Research Board*, 2021. 2675: 1082–1092.
16. Diefenderfer, B. K., D. H. Timm, I. Boz, and B. F. Bowers. *Structural Study of Cold Central Plant Recycling Sections at the National Center for Asphalt Technology (NCAT) Test Track: Phase III*. Report No. 21-R22. Virginia Transportation Research Council, Charlottesville, 2021.
17. Virginia Department of Transportation. Interstate 64 Widening. https://i64widening.org/learn_more/default.asp. Accessed March 18, 2021.
18. ARRA. *Basic Asphalt Recycling Manual*. Asphalt Recycling and Reclaiming Association, Annapolis, MD, 2015.
19. Flintsch, G. W., A. Loulizi, S. D. Diefenderfer, K. A. Galal, and B. K. Diefenderfer. *Asphalt Materials Characterization in Support of Implementation of the Proposed Mechanistic-Empirical Pavement Design Guide*. Report No. 07-CR10. Virginia Transportation Research Council, Charlottesville, 2007.
20. Zhang, Y., L. Wang, W. Zhang, B. Diefenderfer, and Y. Huang. Modified Dynamic Modulus Test and Customized Prediction Model of Asphalt-Treated Drainage Layer Materials for M-E Pavement Design. *International Journal of Pavement Engineering*, Vol. 17, 2016, pp. 818–828.
21. Schwartz, C. W., B. K. Diefenderfer, and B. F. Bowers. *Material Properties of Cold In-Place Recycled and Full-Depth Reclamation Asphalt Concrete*. NCHRP Report 863. National Cooperative Highway Research Program, Washington, D.C., 2017.
22. Willis, J. R., and D. H. Timm. Development of Stochastic Perpetual Pavement Design Criteria. *Journal of the Association of Asphalt Paving Technologists*, Vol. 79, 2010, pp. 561–596.
23. Castro, A. J., N. Tran, M. M. Robbins, D. H. Timm, and C. Wagner. Further Evaluation of Limiting Strain Criteria for Perpetual Asphalt Pavement Design. *Transportation Research Record: Journal of the Transportation Research Board*, 2017. 2640: 41–48.
24. Thompson, M. R., and S. H. Carpenter. Design Principles for Long Lasting HMA Pavements. *Proc., International Society for Asphalt Pavements International Symposium on Design and Construction of Long-Lasting Asphalt Pavements*, Auburn, AL, 2004, pp. 365–384.
25. Francois, A., A. Ali, and Y. Mehta. Evaluating the Impact of Different Types of Stabilized Bases on the Overall Performance of Flexible Pavements. *International Journal of Pavement Engineering*, Vol. 20, 2019, pp. 938–946.
26. Wen, H., B. Muhuthan, J. Wang, X. Li, T. Edil, and J. M. Tunjum. *Characterization of Cementitious Stabilized Layers for Use in Pavement Design and Analysis*. NCHRP Report 789. National Cooperative Highway Research Program, Washington, D.C., 2014.